

An analytical approach for buckling of functionally graded plates

Tahar Hassaine Daouadji^{*1,2} and Belkacem Adim^{1,2}

¹Département de génie civil, Université Ibn Khaldoun Tiaret, BP 78 Zaaroura, 14000 Tiaret, Algérie

²Laboratoire de Géomatique et Développement Durable, Université Ibn Khaldoun Tiaret, Algérie

(Received October 8, 2016, Revised November 2, 2016, Accepted November 2, 2016)

Abstract. In this paper, an efficient and simple refined theory is presented for buckling analysis of functionally graded plates. The theory, which has strong similarity with classical plate theory in many aspects, accounts for a quadratic variation of the transverse shear strains across the thickness and satisfies the zero traction boundary conditions on the top and bottom surfaces of the plate without using shear correction factors. The mechanical properties of functionally graded material are assumed to vary according to a power law distribution of the volume fraction of the constituents. Governing equations are derived from the principle of minimum total potential energy. The closed-form solutions of rectangular plates are obtained. Comparison studies are performed to verify the validity of present results. The effects of loading conditions and variations of power of functionally graded material, modulus ratio, aspect ratio, and thickness ratio on the critical buckling load of functionally graded plates are investigated and discussed.

Keywords: closed-form solution; refined plate theory; buckling analysis; functionally graded plate

1. Introduction

The concept of functionally graded materials FGM were the first introduced in 1984 by a group of material scientists in Japan, as ultrahigh temperature resistant materials for aircraft, space vehicles and other engineering applications. Functionally graded materials are new composite materials in which the micro-structural details are spatially varied through non-uniform distribution of the reinforcement phase. This is achieved by using reinforcement with different properties, sizes and shapes, as well as by interchanging the role of reinforcement and matrix phase in a continuous manner. The result is a microstructure that produces continuous or smooth change on thermal and mechanical properties at the macroscopic or continuum level (Koizumi 1993, Hirai and Chen 1999). Now, FGM are developed for general use as structural components in extremely high temperature environments. Therefore, it is important to study the wave propagation of functionally graded materials structures in terms of non-destructive evaluation and material characterization. Several studies have been performed to analyze the mechanical or the thermal responses of FG plates and shells. A comprehensive review is done by Tanigawa (1995). Reddy

*Corresponding author, Professor, E-mail: daouadjitahar@gmail.com

(2000) has analyzed the static behavior of functionally graded rectangular plates based on his third-order shear deformation plate theory. Cheng and Batra (2000) have related the deflections of a simply supported FG polygonal plate given by the first-order shear deformation theory and third-order shear deformation theory to that of an equivalent homogeneous Kirchhoff plate. The static response of FG plate has been investigated by Tounsi (2013) using a generalized shear deformation theory. In a recent study, Şimşek (2010) has studied the dynamic deflections and the stresses of an FG simply-supported beam subjected to a moving mass by using Euler-Bernoulli, Timoshenko and the parabolic shear deformation beam theory. Tounsi (2013) studied the free vibration of FG beams having different boundary conditions using the classical, the first-order and different higher-order shear deformation beam and plate theories. The functionally graded (FG) plates are commonly used in thermal environments; they can buckle under thermal and mechanical loads. Thus, the buckling analysis of such plates is essential to ensure an efficient and reliable design. Eslami and his co-workers (2006) have treated a series of problems relating to the linear buckling of simply supported rectangular FG plates, with and without imperfections, under mechanical and thermal loads. By using an analytical approach, they obtained closed-form expressions for buckling loads.

The buckling analysis of the square ceramic-metal FG plates with circular holes at the center was presented by Zhao (2009). The effects of the volume fraction index, boundary conditions, hole geometry and hole size on the buckling behavior of FG plates were investigated. Matsunaga (2009) presented a higher order deformation theory for buckling of FG plates. By using the method of power series expansion of displacement components, a set of fundamental equations of rectangular FG plates was derived. Bouazza et al. (2010) investigated the thermo-elastic buckling of FG plates using first shear plate theory. Effects of changing plate characteristics, material composition and volume fraction of constituent materials on the critical temperature difference of FG plate with simply supported edges are also investigated. Zenkour et al. (2010) studied the thermal buckling response of FG plates using sinusoidal shear deformation plate theory. Although the higher-order shear deformation plate theories have been adopted for buckling analysis of FG plates (Najafizadeh 2008, Ait yahia 2015, Attia 2015, belabed 2014, Bellifa 2016, Bouderra 2016, Bourada 2015 and Bounouara 2016), they are not convenience to use due to the higher-order terms introduced into the theory. Therefore, Shimpi (2002) has developed a new refined plate theory that is simple to use.

In this paper, the four-variable refined plate theory developed by Sobhy (2010), Ait Amar Meziane (2014), Bennoun, (2016), Bourada (2015), Hebali (2014), Abdelhak (2016), Cheikh (2016), Loufi (2016), Salima (2016), Ahmed (2016), Bousahla (2014), Hamidi (2015), Houari (2016), Mahi (2015), Tounsi (2016), Zidi (2014), Adim (2016) and Benferhat (2016) has been extended for the first time to the buckling behavior of FGM plates. An Eigen value problem is formulated for a simply supported FGM plates to analyze its thermal and mechanical buckling behaviors. Illustrative examples are given so as to demonstrate the efficacies of the theory. Comparison studies are performed to verify the validity of the present results. The effects of loading conditions and variations of power of function-ally graded material, modulus ratio, aspect ratio, and thickness ratio on the critical buckling load of FGM plates are investigated and discussed.

2. Problem formulation

Consider a rectangular plate of total thickness h as shown in Fig. 1. The plate is made of

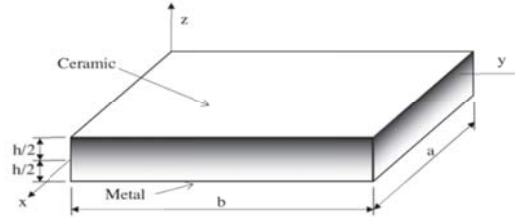


Fig. 1 Geometry of rectangular FG plate and coordinates

isotropic material with material properties varying smoothly in the thickness direction.

2.1 Higher-order plate theory

The displacements of a material point located at (x, y, z) in the plate may be written as

$$u = u_0(x, y) - z \frac{\partial w_0}{\partial x} + \psi(z)\theta_x \tag{1a}$$

$$v = v_0(x, y) - z \frac{\partial w_0}{\partial y} + \psi(z)\theta_y \tag{1b}$$

$$w = w_0(x, y) \tag{1c}$$

Where u, v, w are displacements in the x, y, z directions, u_0, v_0 and w_0 are mid-plane displacements, θ_x and θ_y rotations of the yz and xz planes due to bending, respectively. $\psi(z)$ represents shape function determining the distribution of the transverse shear strains and stresses along the thickness. The displacement field of the classical thin plate theory (CPT) is obtained easily by setting $\psi(z)=0$. The displacement of the first-order shear deformation plate theory FSDPT is obtained by setting $\psi(z)=z$. Also, the displacement of third-order shear deformation plate theory (PSDPT) of Reddy (2000) is obtained by setting

$$\psi(z) = z \left(1 - \frac{4z^2}{3h^2} \right) \tag{2a}$$

The sinusoidal shear deformation plate theory (SSDPT) of Tounsi (2013) is obtained by setting

$$\psi(z) = \frac{h}{\pi} \sin \left(\frac{\pi z}{h} \right) \tag{2b}$$

2.2.1 Assumptions of the refined plate theory

Assumptions of the present model refined plate theory are as follows:

- The displacements are small in comparison with the plate thickness and, therefore, strains involved are infinitesimal.
- The transverse displacement W includes two components of bending w_b , and shear w_s . These components are functions of coordinates x, y , and time t only

$$W(x, y, z) = w_b(x, y) + w_s(x, y) \tag{3a}$$

- The transverse normal stress σ_z is negligible in comparison with in-plane stresses σ_x and σ_y .
- The displacements U in x -direction and V in y -direction consist of extension, bending, and shear components

$$U = u_0 + u_b + u_s, \quad V = v_0 + v_b + v_s \quad (3b)$$

The bending components u_b and v_b are assumed to be similar to the displacements given by the classical plate theory. Therefore, the expression for u_b and v_b can be given as

$$u_b = -z \frac{\partial w_b}{\partial x}, \quad v_b = -z \frac{\partial w_b}{\partial y} \quad (3c)$$

- The shear components u_s and v_s give rise, in conjunction with w_s , to the parabolic variations of shear strains γ_{xz} , γ_{yz} and hence to shear stresses τ_{xz} , τ_{yz} through the thickness of the plate in such a way that shear stresses τ_{xz} , τ_{yz} are zero at the top and bottom faces of the plate. Consequently, the expression for u_s and v_s can be given as

$$u_s = -f(z) \frac{\partial w_s}{\partial x}, \quad v_s = -f(z) \frac{\partial w_s}{\partial y} \quad (3d)$$

2.2.2 Kinematics and constitutive equations

Based on the assumptions made in the preceding section, the displacement field of present theory can be obtained using Eqs. (3a)-(3d) as

$$\begin{aligned} u(x, y, z) &= u_0(x, y) - z \frac{\partial w_b}{\partial x} - f(z) \frac{\partial w_s}{\partial x} \\ v(x, y, z) &= v_0(x, y) - z \frac{\partial w_b}{\partial y} - f(z) \frac{\partial w_s}{\partial y} \\ w(x, y, z) &= w_b(x, y) + w_s(x, y) \end{aligned} \quad (4a)$$

where u_0 and v_0 are the mid-plane displacements of the plate in the x and y direction, respectively; w_b and w_s are the bending and shear components of transverse displacement, respectively, while $f(z)$ represents shape functions determining the distribution of the transverse shear strains and stresses along the thickness and is given as :

- Present model 1 SSDT: The function $f(z)$ is an Sinusoidal shape function (Sinusoidal Shear Deformation Theory)

$$f(z) = z - \sin \frac{\pi z}{h} \quad (4b)$$

- Present model 2 ESDT: The function $f(z)$ is an exponential shape function (Exponential Shear Deformation Theory)

$$f(z) = z - ze^{\left(-2 \frac{z^2}{h^2}\right)} \quad (4c)$$

It should be noted that unlike the first-order shear deformation theory, this theory does not require shear correction factors. The kinematic relations can be obtained as follows

$$\begin{aligned}
 \varepsilon_x &= \varepsilon_x^0 + z k_x^b + f k_x^s \\
 \varepsilon_y &= \varepsilon_y^0 + z k_y^b + f k_y^s \\
 \gamma_{xy} &= \gamma_{xy}^0 + z k_{xy}^b + f k_{xy}^s \\
 \gamma_{yz} &= g \gamma_{yz}^s \\
 \gamma_{xz} &= g \gamma_{xz}^s \\
 \varepsilon_z &= 0
 \end{aligned} \tag{5}$$

Where

$$\begin{aligned}
 \varepsilon_x^0 &= \frac{\partial u_0}{\partial x} + \frac{1}{2} \left(\frac{\partial w_b}{\partial x} + \frac{\partial w_s}{\partial x} \right), & k_x^b &= -\frac{\partial^2 w_b}{\partial x^2}, & k_x^s &= -\frac{\partial^2 w_s}{\partial x^2}, & \varepsilon_y^0 &= \frac{\partial v_0}{\partial y} + \frac{1}{2} \left(\frac{\partial w_b}{\partial y} + \frac{\partial w_s}{\partial y} \right), \\
 k_y^b &= -\frac{\partial^2 w_b}{\partial y^2}, & k_y^s &= -\frac{\partial^2 w_s}{\partial y^2}, & \gamma_{xy}^0 &= \frac{\partial u_0}{\partial y} + \frac{\partial v_0}{\partial x} + \left(\frac{\partial w_b}{\partial x} + \frac{\partial w_s}{\partial x} \right) \left(\frac{\partial w_b}{\partial y} + \frac{\partial w_s}{\partial y} \right), \\
 k_{xy}^b &= -2 \frac{\partial^2 w_b}{\partial x \partial y}, & k_{xy}^s &= -2 \frac{\partial^2 w_s}{\partial x \partial y}, & \gamma_{yz}^s &= \frac{\partial w_s}{\partial y}, & \gamma_{xz}^s &= \frac{\partial w_s}{\partial x}, & f(z) &= z - \psi(z), \\
 g &= 1 - f'(z) \text{ and } f'(z) = \frac{df(z)}{dz}
 \end{aligned} \tag{6}$$

2.2.3 Constitutive relations

Consider a FGM plate made of ceramic and metal, the material properties of FGM such as Young modulus E and coefficient of thermal expansion α are assumed to vary through the plate thickness with a power law distribution of the volume fraction of the two materials as

$$E(z) = E_m + (E_c - E_m) \left(\frac{1}{2} + \frac{z}{h} \right)^p \tag{7a}$$

$$\alpha(z) = \alpha_m + (\alpha_c - \alpha_m) \left(\frac{1}{2} + \frac{z}{h} \right)^p \tag{7b}$$

Where (E_m, α_m) and (E_c, α_c) are the properties of the metal and ceramic, respectively; and p is the volume fraction exponent. The value of p equal to zero represents a fully ceramic plate, whereas infinite p indicates a fully metallic plate. The variation of the combination of ceramic and metal is linear for $p=1$. The variation of Poisson's ratio ν is generally small and it is assumed to be a constant for convenience. The linear constitutive relations of a FG plate can be written as

$$\begin{Bmatrix} \sigma_x \\ \sigma_y \\ \sigma_{xy} \\ \sigma_{yz} \\ \sigma_{xz} \end{Bmatrix} = \begin{bmatrix} Q_{11} & Q_{12} & 0 & 0 & 0 \\ Q_{12} & Q_{22} & 0 & 0 & 0 \\ 0 & 0 & Q_{66} & 0 & 0 \\ 0 & 0 & 0 & Q_{44} & 0 \\ 0 & 0 & 0 & 0 & Q_{55} \end{bmatrix} \begin{Bmatrix} \varepsilon_x - \alpha T \\ \varepsilon_y - \alpha T \\ \gamma_{xy} \\ \gamma_{yz} \\ \gamma_{xz} \end{Bmatrix} \tag{8}$$

Where

$$Q_{11} = Q_{22} = \frac{E(z)}{1 - \nu^2}, \quad Q_{12} = \frac{\nu E(z)}{1 - \nu^2}, \quad Q_{44} = Q_{55} = Q_{66} = \frac{E(z)}{2(1 + \nu)} \tag{9}$$

2.2.4 Governing equations

The strain energy of the plate can be written as

$$U = \frac{1}{2} \int \int \int (\sigma_x \delta(\epsilon_x - \alpha T) + \sigma_y \delta(\epsilon_y - \alpha T) + \tau_{xy} \delta\gamma_{xy} + \tau_{yz} \delta\gamma_{yz} + \tau_{xz} \delta\gamma_{xz}) dx dy dz \quad (10)$$

Substituting Eqs. (5) and (8) into Eq. (10) and integrating through the thickness of the plate, the strain energy of the plate can be rewritten as

$$U = \frac{1}{2} \int_A \{ N_x \epsilon_x^0 + N_y \epsilon_y^0 + N_{xy} \gamma_{xy}^0 + M_x^b k_x^b + M_y^b k_y^b + M_{xy}^b k_{xy}^b + M_x^s k_x^s + M_y^s k_y^s + M_{xy}^s k_{xy}^s + Q_{yz} \gamma_{yz}^s + Q_{xz} \gamma_{xz}^s \} dx dy \quad (11)$$

Where N_i, M_i, Q_j ($i=x, y, xy, j=xz, yz$) are the resultants forces, moments and shear forces, respectively, which are all defined by the following expressions

$$(N_i, M_i^b, M_i^s) = \int_{-h/2}^{h/2} (1, z, f) \sigma_i dz, (i = x, y, xy) \quad \text{and} \quad Q_i = \int_{-h/2}^{h/2} g \sigma_i dz, (i = xz, yz) \quad (12)$$

Substituting Eq. (8) into Eq. (12) and integrating through the thickness of the plate, the stress resultants are given as

$$\begin{Bmatrix} N_x \\ N_y \\ N_{xy} \\ M_x^b \\ M_y^b \\ M_{xy}^b \\ M_x^s \\ M_y^s \\ M_{xy}^s \end{Bmatrix} = \begin{bmatrix} A_{11} & A_{12} & 0 & B_{11} & B_{12} & 0 & B_{11}^s & B_{12}^s & 0 \\ A_{12} & A_{22} & 0 & B_{12} & B_{22} & 0 & B_{12}^s & B_{22}^s & 0 \\ 0 & 0 & A_{66} & 0 & 0 & A_{66} & 0 & 0 & B_{66}^s \\ B_{11} & B_{12} & 0 & D_{11} & D_{12} & 0 & D_{11}^s & D_{12}^s & 0 \\ B_{12} & B_{22} & 0 & D_{12} & D_{22} & 0 & D_{12}^s & D_{22}^s & 0 \\ 0 & 0 & A_{66} & 0 & 0 & D_{66} & 0 & 0 & D_{66}^s \\ B_{11}^s & B_{12}^s & 0 & D_{11}^s & D_{12}^s & 0 & H_{11}^s & H_{12}^s & 0 \\ B_{12}^s & B_{22}^s & 0 & D_{12}^s & D_{22}^s & 0 & H_{12}^s & H_{22}^s & 0 \\ 0 & 0 & B_{66}^s & 0 & 0 & D_{66}^s & 0 & 0 & H_{66}^s \end{bmatrix} \begin{Bmatrix} \epsilon_x^0 \\ \epsilon_y^0 \\ \gamma_{xy}^0 \\ k_x^b \\ k_y^b \\ k_{xy}^b \\ k_x^s \\ k_y^s \\ k_{xy}^s \end{Bmatrix} = \begin{Bmatrix} N_x^T \\ N_y^T \\ 0 \\ M_x^{bT} \\ M_y^{bT} \\ 0 \\ M_x^{sT} \\ M_y^{sT} \\ 0 \end{Bmatrix} \quad (13a)$$

$$\begin{Bmatrix} Q_{yz} \\ Q_{xz} \end{Bmatrix} = \begin{bmatrix} A_{44}^s & 0 \\ 0 & A_{55}^s \end{bmatrix} \begin{Bmatrix} \gamma_{yz}^s \\ \gamma_{xz}^s \end{Bmatrix} \quad (13b)$$

Where A_{ij}, B_{ij} , etc., are the plate stiffness, defined by

$$(A_{ij}, B_{ij}, D_{ij}, B_{ij}^s, D_{ij}^s, H_{ij}^s) = \int_{-h/2}^{h/2} \bar{Q}_{ij} (1, z, z^2, f(z), zf(z), f^2(z)) dz, \quad (i, j) = (1,2,6) \quad (14a)$$

$$A_{ij}^s = \int_{-h/2}^{h/2} \bar{Q}_{ij} [g(z)] dz, \quad (i, j) = (4,5) \quad (14b)$$

The stress and moment resultants, $N_x^T = N_y^T$, $M_x^{bt} = M_y^{bt}$, and $M_x^{st} = M_y^{st}$ due to thermal loading are defined by

$$\begin{Bmatrix} N_x^T \\ M_x^{bT} \\ M_x^{sT} \end{Bmatrix} = \int_{-h/2}^{h/2} \frac{E(z)}{1-\nu} \alpha(z) T \begin{Bmatrix} 1 \\ z \\ f(z) \end{Bmatrix} dz \quad (15)$$

The work done by applied forces can be written as

$$V = \frac{1}{2} \int_A \left[N_x \frac{\partial^2 (w_b + w_s)}{\partial x^2} + N_y \frac{\partial^2 (w_b + w_s)}{\partial y^2} + 2N_{xy} \frac{\partial^2 (w_b + w_s)}{\partial x \partial y} \right] dx dy \quad (16)$$

Where N_x ; N_y ; N_{xy} are in-plane pre-buckling forces.

The principle of minimum total potential energy is used herein to derive the governing equation. The principle can be stated in analytical form as (Tounsi 2013)

$$\delta(U + V) = 0 \quad (17)$$

The stability equations of the plate may be derived by the adjacent equilibrium criterion. Assume that the equilibrium state of the FG plate under thermal loads is defined in terms of the displacement components $(u_0^0, v_0^0, w_b^0, w_s^0)$. The displacement components of a neighboring stable state differ by $(u_0^1, v_0^1, w_b^1, w_s^1)$ with respect to the equilibrium position. Thus, the total displacements of a neighboring state are

$$u_0 = u_0^0 + u_0^1, \quad v_0 = v_0^0 + v_0^1, \quad w_b = w_b^0 + w_b^1, \quad w_s = w_s^0 + w_s^1 \quad (18)$$

Where the superscript 1 refers to the state of stability and the superscript 0 refers to the state of equilibrium conditions.

Substituting Eqs. (4) and (18) into Eq. (17) and integrating by parts and then equating the coefficients of $\delta u_0^1, \delta v_0^1, \delta w_b^1, \delta w_s^1$ to zero, separately, the governing stability equations are obtained for the shear deformation plate theories as

$$\begin{aligned} \frac{\partial N_x^1}{\partial x} + \frac{\partial N_{xy}^1}{\partial y} &= 0 \\ \frac{\partial N_{xy}^1}{\partial x} + \frac{\partial N_y^1}{\partial y} &= 0 \\ \frac{\partial^2 M_x^{b1}}{\partial x^2} + 2 \frac{\partial^2 M_{xy}^{b1}}{\partial x \partial y} + \frac{\partial^2 M_y^{b1}}{\partial y^2} + \overline{N_T} + \overline{N_M} &= 0 \\ \frac{\partial^2 M_x^{s1}}{\partial x^2} + 2 \frac{\partial^2 M_{xy}^{s1}}{\partial x \partial y} + \frac{\partial^2 M_y^{s1}}{\partial y^2} + \frac{\partial Q_{xz}^1}{\partial x} + \frac{\partial Q_{yz}^1}{\partial y} + \overline{N_T} + \overline{N_M} &= 0 \end{aligned} \quad (19)$$

With

$$\overline{N_M} = N_x \frac{\partial^2 (w_b^1 + w_s^1)}{\partial x^2} + N_y \frac{\partial^2 (w_b^1 + w_s^1)}{\partial y^2} + 2N_{xy} \frac{\partial^2 (w_b^1 + w_s^1)}{\partial x \partial y} \quad (20)$$

And

$$\overline{N_T} = \left[N_x^0 \frac{\partial^2 (w_b^1 + w_s^1)}{\partial x^2} + N_y^0 \frac{\partial^2 (w_b^1 + w_s^1)}{\partial y^2} \right] \quad (21)$$

Where the terms N_x^0 and N_y^0 are the pre-buckling force resultants obtained as

$$N_x^0 = N_y^0 = - \int_{-\frac{h}{2}}^{\frac{h}{2}} \frac{\alpha(z) E(z) T}{1-\nu} dz \quad (22)$$

Trigonometric solution for simply supported FGM plates

Rectangular plates are generally classified in accordance with the type of support used. We are here concerned with the exact solution of Eqs. (19) for a simply supported FGM plate. The following boundary conditions are imposed for the present four variable refined plate theory at the side edges

$$v_0^1 = w_b^1 = w_s^1 = \frac{\partial w_s^1}{\partial y} = N_x^1 = M_x^{b1} = M_x^{s1} = 0 \quad \text{at} \quad x = 0, a \quad (23a)$$

$$u_0^1 = w_b^1 = w_s^1 = \frac{\partial w_s^1}{\partial x} = N_y^1 = M_y^{b1} = M_y^{s1} = 0 \quad \text{at} \quad y = 0, b \quad (23b)$$

The following approximate solution is seen to satisfy both the differential equation and the boundary conditions

$$\begin{Bmatrix} u_0^1 \\ v_0^1 \\ w_b^1 \\ w_s^1 \end{Bmatrix} = \sum_{m=1}^{\infty} \sum_{n=1}^{\infty} \begin{Bmatrix} U_{mn}^1 \cos(\lambda x) \sin(\mu y) \\ V_{mn}^1 \sin(\lambda x) \cos(\mu y) \\ W_{bmn}^1 \sin(\lambda x) \sin(\mu y) \\ W_{smn}^1 \sin(\lambda x) \sin(\mu y) \end{Bmatrix} \quad (24)$$

Where U_{mn}^1 , V_{mn}^1 , W_{bmn}^1 and W_{smn}^1 are arbitrary parameters to be determined, $\lambda = m\pi/a$ and $\mu = n\pi/b$ and m and n are mode numbers. Substituting Eq. (24) into Eq. (19), one obtains

$$[K] \{\Delta\} = \{0\} \quad (25)$$

Where $\{\Delta\}$ denotes the column

$$\{\Delta\} = \{U_{mn}^1, V_{mn}^1, W_{bmn}^1, W_{smn}^1\}^t \quad (26)$$

And $[K]$ is the symmetric matrix given by

$$[K] = \begin{bmatrix} a_{11} & a_{12} & a_{13} & a_{14} \\ a_{12} & a_{22} & a_{23} & a_{24} \\ a_{13} & a_{23} & a_{33} + k & a_{34} + k \\ a_{14} & a_{24} & a_{34} + k & a_{44} + k \end{bmatrix} \quad (27)$$

In which

$$\begin{aligned}
 a_{11} &= -(A_{11}\lambda^2 + A_{66}\mu^2) \\
 a_{12} &= -\lambda\mu(A_{12} + A_{66}) \\
 a_{13} &= \lambda[B_{11}\lambda^2 + (B_{12} + 2B_{66})\mu^2] \\
 a_{14} &= \lambda[B_{11}^s\lambda^2 + (B_{12}^s + 2B_{66}^s)\mu^2] \\
 a_{22} &= -(A_{66}\lambda^2 + A_{22}\mu^2) \\
 a_{23} &= \mu[(B_{12} + 2B_{66})\lambda^2 + B_{22}\mu^2] \\
 a_{24} &= \mu[(B_{12}^s + 2B_{66}^s)\lambda^2 + B_{22}^s\mu^2] \\
 a_{33} &= -(D_{11}\lambda^4 + 2(D_{12} + 2D_{66})\lambda^2\mu^2 + D_{22}\mu^4 + N_x^0\lambda^2 + N_y^0\mu^2) \\
 a_{34} &= -(D_{11}^s\lambda^4 + 2(D_{12}^s + 2D_{66}^s)\lambda^2\mu^2 + D_{22}^s\mu^4 + N_x^0\lambda^2 + N_y^0\mu^2) \\
 a_{44} &= -(H_{11}^s\lambda^4 + 2(H_{12}^s + 2H_{66}^s)\lambda^2\mu^2 + H_{22}^s\mu^4 + A_{55}^s\lambda^2 + A_{44}^s\mu^2 + N_x^0\lambda^2 + N_y^0\mu^2) \\
 k &= N_{cr}(\gamma_1\lambda^2 + \gamma_2\mu^2)
 \end{aligned} \tag{28}$$

By applying the static condensation approach to eliminate the coefficients associated with the in-plane displacements, Eq. (25) can be rewritten as

$$\begin{bmatrix} [K^{11}] & [K^{12}] \\ [K^{12}]^T & [K^{22}] \end{bmatrix} \begin{Bmatrix} \Delta^1 \\ \Delta^2 \end{Bmatrix} = \begin{Bmatrix} 0 \\ 0 \end{Bmatrix} \tag{29}$$

Where

$$[K^{11}] = \begin{bmatrix} a_{11} & a_{12} \\ a_{12} & a_{22} \end{bmatrix}, \quad [K^{12}] = \begin{bmatrix} a_{13} & a_{14} \\ a_{23} & a_{24} \end{bmatrix}, \quad [K^{22}] = \begin{bmatrix} a_{33} & a_{34} \\ a_{34} & a_{44} \end{bmatrix} \tag{30a}$$

$$\Delta^1 = \begin{Bmatrix} U_{mn}^1 \\ V_{mn}^1 \end{Bmatrix}, \quad \Delta^2 = \begin{Bmatrix} W_{bmn}^1 \\ W_{smn}^1 \end{Bmatrix} \tag{30b}$$

Eq. (29) represents a pair of two matrix equations

$$[K^{11}]\Delta^1 + [K^{12}]\Delta^2 = 0 \tag{31a}$$

$$[K^{12}]^T\Delta^1 + [K^{22}]\Delta^2 = 0 \tag{31b}$$

Solving Eq. (31a) for Δ^1 and then substituting the result into Eq. (31b), the following equation is obtained

$$[\bar{K}^{22}]\Delta^2 = 0 \tag{32}$$

Where

$$[\bar{K}^{22}] = [K^{22}] - [K^{12}]^T [K^{11}]^{-1} [K^{12}] = \begin{bmatrix} \bar{a}_{33} & \bar{a}_{34} \\ \bar{a}_{43} & \bar{a}_{44} \end{bmatrix} \tag{33a}$$

And

$$\begin{aligned}
\bar{a}_{33} &= a_{33} - a_{13} \frac{b_1}{b_0} - a_{23} \frac{b_2}{b_0}, & \bar{a}_{34} &= a_{34} - a_{14} \frac{b_1}{b_0} - a_{24} \frac{b_2}{b_0} \\
\bar{a}_{43} &= a_{34} - a_{13} \frac{b_3}{b_0} - a_{23} \frac{b_4}{b_0}, & \bar{a}_{44} &= a_{44} - a_{14} \frac{b_3}{b_0} - a_{24} \frac{b_4}{b_0} \\
b_0 &= a_{11} a_{22} - a_{12}^2, & b_1 &= a_{13} a_{22} - a_{12} a_{23}, & b_2 &= a_{11} a_{23} - a_{12} a_{13} \\
b_3 &= a_{14} a_{22} - a_{12} a_{24}, & b_4 &= a_{11} a_{24} - a_{12} a_{14}
\end{aligned} \tag{33b}$$

For nontrivial solution, the determinant of the coefficient matrix in Eq. (32) must be zero. This gives the following expressions:

For the thermal buckling load

$$N_x^0 = N_y^0 = \frac{1}{\lambda^2 + \mu^2} \frac{\bar{a}_{33}\bar{a}_{44} - \bar{a}_{34}\bar{a}_{43}}{\bar{a}_{33} + \bar{a}_{44} - \bar{a}_{34} - \bar{a}_{43}} \tag{34}$$

For mechanical buckling load

$$N_{cr}(m, n) = \frac{-1}{\gamma_1 \lambda^2 + \gamma_2 \mu^2} \frac{\bar{a}_{33}\bar{a}_{44} - \bar{a}_{34}\bar{a}_{43}}{\bar{a}_{33} + \bar{a}_{44} - \bar{a}_{34} - \bar{a}_{43}} \tag{35}$$

Buckling of FG Plates under Uniform Temperature Rise

The plate initial temperature is assumed to be T_i . The temperature is uniformly raised to a final value T_f in which the plate buckles. The temperature change is $\Delta T = T_f - T_i$. Using this distribution of temperature, the critical buckling temperature change ΔT_{cr} becomes by using Eqs. (22) and (34)

$$\Delta T_{cr} = \frac{1}{\bar{\beta}_1(\lambda^2 + \mu^2)} \frac{\bar{a}_{33}\bar{a}_{44} - \bar{a}_{34}\bar{a}_{43}}{\bar{a}_{33} + \bar{a}_{44} - \bar{a}_{34} - \bar{a}_{43}} \tag{36a}$$

Where

$$\bar{\beta}_1 = - \int_{-h/2}^{h/2} \frac{\alpha(z)E(z)}{1-\nu} dz \tag{36b}$$

For the case of CPT, the expression of the critical buckling temperature change ΔT_{cr} can be simplified by setting the shear component of transverse displacement to zero ($w_s=0$) as

$$\Delta T_{cr} = \frac{\bar{a}_{33}}{\bar{\beta}_1(\lambda^2 + \mu^2)} \tag{37}$$

Buckling of FG Plates Subjected to Graded Temperature Change across the Thickness

We assume that the temperature of the top surface is T_t and the temperature varies from T_t , according to the power law variation through-the-thickness, to the bottom surface temperature T_b in which the plate buckles. In this case, the temperature through-the-thickness is given by

$$T(z) = \Delta T \left(\frac{z}{h} + \frac{1}{2} \right)^\gamma + T_t \quad (38)$$

Where the buckling temperature difference $\Delta T = T_b - T_t$ and γ is the temperature exponent ($0 < \gamma < \infty$). Note that the value of γ equal to unity represents a linear temperature change across the thickness. While the value of γ excluding unity represents a non-linear temperature change through-the-thickness. Similar to the previous loading case, the critical buckling temperature change ΔT_{cr} becomes by using Eqs. (22) and (34)

$$\Delta T_{cr} = \frac{\bar{a}_{33} \bar{a}_{44} - \bar{a}_{34} \bar{a}_{43} + T_t \bar{\beta}_1 (\lambda^2 + \mu^2) (\bar{a}_{33} + \bar{a}_{44} - \bar{a}_{34} - \bar{a}_{43})}{\bar{\beta}_2 (\lambda^2 + \mu^2) (\bar{a}_{33} + \bar{a}_{44} - \bar{a}_{34} - \bar{a}_{43})} \quad (39a)$$

Where

$$\bar{\beta}_2 = - \int_{-h/2}^{h/2} \frac{\alpha(z) E(z)}{1 - \nu} \left(\frac{z}{h} + \frac{1}{2} \right)^\gamma dz \quad (39b)$$

For the case of CPT, the expression of the critical buckling temperature change ΔT_{cr} is obtained as follows

$$\Delta T_{cr} = \frac{\bar{a}_{33} + T_t \bar{\beta}_1 (\lambda^2 + \mu^2)}{\bar{\beta}_2 (\lambda^2 + \mu^2)} \quad (40)$$

3. Results and discussion

In this section, various numerical examples are presented and discussed for verifying the accuracy and efficiency of the present theory in predicting buckling stability of simply supported FG plates under mechanical and uniform, linear and nonlinear thermal loadings through the thickness. For the verification purpose, the results obtained by the present four variable refined plate theory are compared with the existing data in the literature. It is assumed that the functionally graded plate is made of a mixture of aluminum and alumina. The Young modulus and coefficient of thermal expansion for aluminum are $E_m = 70$ GPa, $\alpha_m = 23 \times 10^{-6}/^\circ\text{C}$ and for alumina are $E_c = 380$ GPa, $\alpha_c = 7.4 \times 10^{-6}/^\circ\text{C}$, respectively. For the linear and non-linear temperature rises through the thickness, the temperature rises 5°C in the metal-rich surface of the plate (i.e., $T_m = 5^\circ\text{C}$). We will assume in all analyzed cases (unless otherwise stated) that $a/b = 2$, $a/h = 10$, and $\gamma = 3$.

3.1 Mechanical buckling load

This study is done on the mechanical buckling of FGM plates subjected to axial and biaxial mechanical loads. Based on two shear refined functions of four unknowns, the plate is assumed simply supported. The various non-dimensional parameters used are

$$\bar{N} = \frac{N a^2}{E_m h^3}, \quad \hat{N} = \frac{N_{cr} b^2}{\pi^2 D}, \quad D = \frac{E h^3}{12(1 - \nu^2)} \quad (41)$$

Table 1 shows the results of the critical buckling load of an isotropic plate under different types of loads depending on aspect ratio a/b and the thickness ratio h/b . This table shows the comparison of critical buckling loads obtained by the present refined theories (present1 and present2) with those given by the higher order theories FSDT and Reddy (2000). These theories 1 and 2 show a very good agreement with the high-order theories FSDT and Reddy (2000) for functionally graded plates, where the shear effect has a major importance. It should be noted that these theories involve only four unknowns against five unknowns in higher order theories Reddy (2000) and FSDT, and this without using shear correction factors. And even, more the plate becomes very thick, more the difference between the results obtained by the first-order theory and those theories FSDT high order (present1, present2 and Reddy 2000) increases. This is due to the incorrect insertion of the shearing effect by the first order theory FSDT.

Table 1 Variation of the critical buckling loads \hat{N} of isotropic plates under different types of loading with ($P=0$)

a/b	h/b	Theory	Load type		
			-1,0	0,-1	-1,-1
1	0.1	FSDT	3.7865	3.7865	1.8932
		Reddy (2000)	3.7866	3.7866	1.8933
		Present Theory 1	3.7869	3.7869	1.8934
		Present Theory 2	3.7878	3.7878	1.8939
	0.2	FSDT	3.2637	3.2637	1.6319
		Reddy (2000)	3.2653	3.2653	1.6327
		Present Theory 1	3.2665	3.2665	1.6332
		Present Theory 2	3.2697	3.2697	1.6348
	0.3	FSDT	2.6533	2.6533	1.3266
		Reddy (2000)	2.6586	2.6586	1.3293
		Present Theory 1	2.6611	2.6611	1.3305
		Present Theory 2	2.6665	2.6665	1.3332
0.4	FSDT	1.9196	1.9196	1.0513	
	Reddy (2000)	1.9550	1.9550	1.0567	
	Present Theory 1	1.9651	1.9632	1.0585	
	Present Theory 2	1.9663	1.9666	1.0622	
1.5	0.1	FSDT	4.0250	2.0048	1.3879
		Reddy (2000)	4.0253	2.0048	1.3879
		Present Theory 1	4.0258	2.0049	1.3880
		Present Theory 2	4.0271	2.0052	1.3882
	0.2	FSDT	3.3048	1.7941	1.2421
		Reddy (2000)	3.3077	1.7946	1.2424
		Present Theory 1	3.3096	1.7950	1.2427
		Present Theory 2	3.3139	1.7963	1.2436
	0.3	FSDT	2.5457	1.5267	1.0570

Table 1 Continued

a/b	h/b	Theory	Load type		
			-1,0	0,-1	-1,-1
1.5	0.3	Reddy (2000)	2.5545	1.5285	1.0582
		Present Theory 1	2.5580	1.5295	1.0588
		Present Theory 2	2.5650	1.5318	1.0605
	0.4	FSDT	1.9196	1.2632	0.8745
		Reddy (2000)	1.9421	1.2670	0.8772
		Present Theory 1	1.9473	1.2686	0.8782
	Present Theory 2	1.9563	1.2718	0.8805	
2	0.1	FSDT	3.7865	1.5093	1.2074
		Reddy (2000)	3.7866	1.5093	1.2075
		Present Theory 1	3.7869	1.5094	1.2075
		Present Theory 2	3.7879	1.5096	1.2077
	0.2	FSDT	3.2637	1.3694	1.0955
		Reddy (2000)	3.2654	1.3697	1.0958
		Present Theory 1	3.2666	1.3700	1.0960
		Present Theory 2	3.2697	1.3708	1.0966
	0.3	FSDT	2.5726	1.1862	0.9490
		Reddy (2000)	2.5839	1.1873	0.9490
		Present Theory 1	2.5882	1.1879	0.9503
		Present Theory 2	2.5964	1.1894	0.9515
0.4	FSDT	1.9034	0.9991	0.7992	
	Reddy (2000)	1.9230	1.0015	0.8012	
	Present Theory 1	1.9292	1.0025	0.8020	
	Present Theory 2	1.9394	1.0047	0.8038	

Table 2 Variation of the critical buckling loads of simply supported rectangular FGM plates ($a/b=0.5, p=1$)

(γ_1, γ_2)	Theory	a/h					
		5	10	20	30	40	50
(-1,0)	FSDT	3.7382	3.8000	3.8158	3.8188	3.8198	3.8203
	Reddy (2000)	3.4163	3.7110	3.7930	3.8086	3.8140	3.8166
	Present Theory 1	3.4170	3.7112	3.7930	3.8086	3.8141	3.8166
	Present Theory 2	3.4188	3.7117	3.7932	3.8086	3.8141	3.8168
(-1,-1)	FSDT	2.9906	3.0400	3.0526	3.0550	3.0558	3.0562
	Reddy (2000)	2.7330	2.9688	3.0344	3.0468	3.0512	3.0533
	Present Theory 1	2.7336	2.9690	3.0344	3.0469	3.0512	3.0533
	Present Theory 2	2.7350	2.9694	3.0345	3.0469	3.0513	3.0533
(-1,1)	FSDT	4.9843	5.0667	5.0878	5.0917	5.0931	5.0937
	Reddy (2000)	4.5551	4.9481	5.0573	5.0781	5.0854	5.0888
	Present Theory 1	4.5560	4.9483	5.0574	5.0781	5.0854	5.0888
	Present Theory 2	4.5584	4.9490	5.0576	5.0782	5.0855	5.0888

Table 2 shows the variation of the critical buckling loads of simply supported functionally graded rectangular plates (FGM) in various types of mechanical loads (axial or biaxial) using different shear theories, where the variation of volume fraction of the components is linear ($P=1$). It is clear that the results obtained by these refined theories 1 and 2 are in excellent convergence with those obtained by high-order theories (Reddy 2000 and FSDT) for all values of the thickness ratio a/h . From this comparison we can see that the critical buckling load increases by increasing the thickness ratio a/h , in other words, from the thin plate to thick one.

Table 3 Variation of the critical buckling load \bar{N} of a simply supported plate under uniaxial compression ($\gamma_1=-1, \gamma_2=0$)

a/b	Theory	a/h	P				
			ceramic	1	5	20	metal
0.5	Present Theory 1	5	6.7218 ^b	3.4170 ^b	2.1459 ^b	1.7126 ^b	2.7663 ^b
		20	7.5993 ^b	3.7930 ^b	2.4942 ^b	2.0255 ^b	3.9627 ^b
		100	7.6635 ^b	3.8200 ^b	2.5204 ^b	2.0277 ^b	4.0763 ^b
	Present Theory 2	5	6.7259 ^b	3.4188 ^b	2.1446 ^b	1.7148 ^b	2.7716 ^b
		20	7.5996 ^b	3.7932 ^b	2.4940 ^b	2.0057 ^b	3.9632 ^b
		100	7.6635 ^b	3.8200 ^b	2.5204 ^b	2.0277 ^b	4.0764 ^b
1	Present Theory 1	5	16.0271 ^b	8.2272 ^b	5.0448 ^b	4.0112 ^b	3.6244 ^b
		20	19.3531 ^b	9.6676 ^b	6.3438 ^b	5.0991 ^b	5.4568 ^b
		100	19.6145 ^b	9.7775 ^b	6.4506 ^b	5.1896 ^b	5.6408 ^b
	Present Theory 2	5	16.0424 ^b	8.2340 ^b	5.0407 ^b	4.0188 ^b	3.6325 ^b
		20	19.3543 ^b	9.6681 ^b	6.3433 ^b	5.0998 ^b	5.4577 ^b
		100	19.6145 ^b	9.7775 ^b	6.4506 ^b	5.1897 ^b	5.6409 ^b
1.5	Present Theory 1	5	28.2386 ^a	15.0531 ^a	8.4506 ^a	6.6304 ^a	5.2018 ^a
		20	45.8960 ^a	23.0298 ^a	14.9408 ^a	11.9869 ^a	8.4545 ^a
		100	47.8298 ^a	23.8469 ^a	15.7252 ^a	12.6502 ^a	8.8107 ^a
	Present Theory 2	5	28.3163 ^a	15.0904 ^a	8.4445 ^a	6.6628 ^a	5.2161 ^a
		20	45.9050 ^a	23.0337 ^a	14.9373 ^a	11.9919 ^a	8.4561 ^a
		100	47.8302 ^a	23.8471 ^a	15.7251 ^a	12.6504 ^a	8.8108 ^a

^a - the mode of the plate is $(m, n) = (2, 1)$. ^b - the mode of the plate is $(m, n) = (1, 1)$

Table 4 Variation of the critical buckling load \bar{N} of a simply supported plate under biaxial compression ($\gamma_1=-1, \gamma_2=-1$)

a/b	Theory	a/h	P				
			ceramic	1	5	20	metal
0.5	Present Theory 1	5	5.3774	2.7336	1.7167	1.3701	0.9905
		20	6.0795	3.0344	1.9953	1.6044	1.1199
		100	6.1308	3.0560	2.0163	1.6222	1.1293
	Present Theory 2	5	5.3807	2.7350	1.7157	1.3718	0.9911
		20	6.0797	3.0345	1.9952	1.6045	1.1199

Table 4 Continued

a/b	Theory	a/h	P				
			ceramic	1	5	20	metal
0.5	Present Theory 2	100	6.1308	3.0560	2.0163	1.6222	1.1293
		5	8.0135	4.1136	2.5224	2.0056	1.4761
1	Present Theory 1	20	9.6765	4.8338	3.1719	2.5495	1.7825
		100	9.8072	4.8887	3.2253	2.5948	1.8066
		5	8.0212	4.1170	2.5203	2.0094	1.4775
	Present Theory 2	20	9.6771	4.8340	3.1716	2.5499	1.7826
		100	9.8072	4.8887	3.2253	2.5948	1.8066
		5	11.6896	6.0834	3.6097	2.8587	2.1533
1.5	Present Theory 1	20	15.5892	7.7978	5.0994	4.0966	2.8717
		100	15.9312	7.9419	5.2388	4.2146	2.9346
		5	11.7072	6.0915	3.6063	2.8639	2.1566
	Present Theory 2	20	15.5908	7.7985	5.0987	4.0475	2.8719
		100	15.9312	7.9419	5.2388	4.2147	2.9347
		5	11.6896	6.0834	3.6097	2.8587	2.1533

Table 5 Variation of the critical buckling load \bar{N} of a simply supported plate under biaxial load, compression and tension ($\gamma_1=-1, \gamma_2=1$)

a/b	Theory	a/h	p				
			ceramic	1	5	20	metal
0.5	Present Theory 1	5	8.9624 ^b	4.5560 ^b	2.8612 ^b	2.2835 ^b	1.6509 ^b
		20	10.1325 ^b	5.0574 ^b	3.3256 ^b	2.6740 ^b	1.8665 ^b
		100	10.2180 ^b	5.0933 ^b	3.3606 ^b	2.7037 ^b	1.8822 ^b
	Present Theory 2	5	8.9679 ^b	4.5584 ^b	2.8595 ^b	2.2864 ^b	1.6519 ^b
		20	10.1329 ^b	5.056 ^b	3.3254 ^b	2.6742 ^b	1.8665 ^b
		100	10.2180 ^b	5.0933 ^b	3.3606 ^b	2.7037 ^b	1.8822 ^b
1	Present Theory 1	5	26.2338 ^a	13.8618 ^a	7.9389 ^a	6.2473 ^a	4.8325 ^a
		20	39.4971 ^a	19.7933 ^a	12.8833 ^a	10.3417 ^a	7.2757 ^a
		100	40.8291 ^a	20.3554 ^a	13.4247 ^a	10.7998 ^a	7.5211 ^a
	Present Theory 2	5	26.2928 ^a	13.8896 ^a	7.9318 ^a	6.2729 ^a	4.8434 ^a
		20	39.5033 ^a	19.7960 ^a	12.8808 ^a	10.3452 ^a	7.2769 ^a
		100	40.8294 ^a	20.3555 ^a	13.4246 ^a	10.8000 ^a	7.5212 ^a
1.5	Present Theory 1	5	64.5454 ^a	34.4071 ^a	19.3158 ^a	15.1552 ^a	11.8899 ^a
		20	104.9052 ^a	52.6397 ^a	34.1505 ^a	27.3986 ^a	19.3246 ^a
		100	109.3253 ^a	54.5073 ^a	35.9434 ^a	28.9149 ^a	20.1388 ^a
	Present Theory 2	5	64.7231 ^a	34.4923 ^a	19.3017 ^a	15.2293 ^a	11.9226 ^a
		20	104.9258 ^a	52.6484 ^a	34.1425 ^a	27.4101 ^a	19.3284 ^a
		100	109.3262 ^a	54.5077 ^a	35.9431 ^a	28.9154 ^a	20.1390 ^a

^a- the mode of the plate is (m, n) = (2, 1). ^b- the mode of the plate is (m, n) = (1, 1)

Table 6 Critical buckling temperature of FGM plate under uniform temperature rise for different values of power law index P and aspect ratio a/b with $a/h=100$

P	Theory	$a/b=1$	$a/b=2$	$a/b=3$	$a/b=4$	$a/b=5$
Ceramic	CPT	17.0991	42.7477	85.4955	145.3424	222.2883
	Reddy (2000)	17.0894	42.6875	85.2551	144.6490	220.6706
	Zenkour (2010)	17.0894	42.6876	85.2554	144.6500	220.6729
	Present Theory 1	17.0894	42.6876	85.2554	144.6500	220.6729
	Present Theory 2	17.0895	42.6879	85.2565	144.6531	220.6802
1	CPT	7.9437	19.8594	39.7188	67.5220	103.2690
	Reddy (2000)	7.9400	19.8358	39.6248	67.2506	102.6356
	Zenkour (2010)	7.9400	19.8369	39.6249	67.2510	102.6365
	Present Theory 1	7.9400	19.8359	39.6249	67.2510	102.6365
	Present Theory 2	7.9400	19.8360	39.6253	67.2523	102.6394
2	CPT	7.0426	17.6065	35.2130	59.8621	91.5538
	Reddy (2000)	7.0390	17.5840	35.1234	59.6037	90.9508
	Zenkour (2010)	7.0390	17.5840	35.1233	59.6034	90.9501
	Present Theory 1	7.0390	17.5840	35.1233	59.6034	90.9501
	Present Theory 2	7.0390	17.5841	35.1235	59.6039	90.9514
5	CPT	7.2657	18.1642	36.3285	61.7585	94.4542
	Reddy (2000)	7.2606	18.1327	36.2025	61.3951	93.6069
	Zenkour (2010)	7.2606	18.1324	36.2014	61.3921	93.5999
	Present Theory 1	7.2606	18.1324	36.2014	61.3921	93.5999
	Present Theory 2	7.2605	18.1323	36.2008	61.3904	93.5959
10	CPT	7.4692	18.6731	37.3463	63.4888	97.1005
	Reddy (2000)	7.4634	18.6366	37.2006	63.0687	96.1213
	Zenkour (2010)	7.4634	18.6365	37.2001	63.0673	96.1183
	Present Theory 1	7.4634	18.6365	37.2001	63.0673	96.1183
	Present Theory 2	7.4634	18.6365	37.2002	63.0677	96.1191
Metal	CPT	5.5014	13.7536	27.5072	46.7623	71.5188
	Reddy (2000)	5.4983	13.7342	27.4299	46.5392	70.9983
	Zenkour (2010)	5.4983	13.7342	27.4300	46.5395	70.9991
	Present Theory 1	5.4983	13.7342	27.4300	46.5395	70.9991
	Present Theory 2	5.4983	13.7343	27.4303	46.5405	71.0014

Table 7 Critical buckling temperature of square FGM plate under uniform temperature rise for different values of power law index k and side-to-thickness ratio a/h

P	Theory	$a/h=10$	$a/h=20$	$a/h=40$	$a/h=60$	$a/h=80$	$a/h=100$
Ceramic	CPT	1709.9106	427.4776	106.8694	47.4975	26.7173	17.0991
	Reddy (2000)	1618.6819	421.5352	106.4940	47.4232	26.6938	17.0894
	Zenkour (2010)	1618.8200	421.5439	106.4946	47.4233	26.6938	17.0894
	Present Theory 1	1618.8200	421.5439	106.4946	47.4233	26.6938	17.0894
	Present Theory 2	1619.2253	421.5706	106.4962	47.4236	26.6939	17.0895

Table 7 Continued

P	Theory	$a/h=10$	$a/h=20$	$a/h=40$	$a/h=60$	$a/h=80$	$a/h=100$
1	CPT	728.9363	183.7513	46.6355	21.0055	11.9571	7.7348
	Reddy (2000)	758.3956	196.2652	49.5016	22.0369	12.4029	7.9400
	Zenkour (2010)	758.4505	196.2686	49.5019	22.0370	12.4029	7.9400
	Present Theory 1	758.4506	196.2686	49.5019	22.0370	12.4029	7.9400
	Present Theory 2	758.6117	196.2791	49.5025	22.0371	12.4029	7.9400
2	CPT	610.4694	155.4493	40.1353	18.3323	10.5570	6.8958
	Reddy (2000)	670.1092	173.8487	43.8763	19.5351	10.9953	7.0390
	Zenkour (2010)	670.0769	173.8462	43.8762	19.5350	10.9952	7.0390
	Present Theory 1	670.0769	173.8462	43.8762	19.5350	10.9952	7.0390
	Present Theory 2	670.1544	173.8511	43.8765	19.5351	10.9953	7.0390
5	CPT	647.7594	165.3567	42.8152	19.5758	11.2718	7.3568
	Reddy (2000)	679.3104	178.5353	45.2139	20.1435	11.3403	7.2606
	Zenkour (2010)	670.0769	173.8462	43.8762	19.5350	10.9952	7.0390
	Present Theory 1	678.9491	178.5098	45.2122	20.1432	11.3402	7.2606
	Present Theory 2	678.7519	178.4956	45.2113	20.1430	11.3401	7.2605
10	CPT	704.2150	178.3669	45.5614	20.5966	11.7463	7.6037
	Reddy (2000)	692.6947	183.1444	46.4554	20.7029	11.6564	7.4634
	Zenkour (2010)	692.5441	183.1338	46.4547	20.7027	11.6564	7.4634
	Present Theory 1	692.5442	183.1333	46.4547	20.7027	11.6564	7.4634
	Present Theory 2	692.5976	183.1364	46.4548	20.7028	11.6564	7.4634
Metal	CPT	550.1451	137.5362	34.3840	15.2818	8.5960	5.5014
	Reddy (2000)	520.7933	135.6243	34.2633	15.2579	8.5884	5.4983
	Zenkour (2010)	520.8377	135.6271	34.2634	15.2579	8.5884	5.4983
	Present Theory 1	520.8377	135.6271	34.2634	15.2579	8.5884	5.4983
	Present Theory 2	520.9681	135.6357	34.2640	15.2580	8.5884	5.4983

Table 8 Critical buckling temperature of FGM plate under linear temperature rise for different values of power law index P and aspect ratio a/b with $a/h=100$

P	Theory	$a/b=1$	$a/b=2$	$a/b=3$	$a/b=4$	$a/b=5$
Ceramic 0	CPT	24.1982	75.4955	160.9910	280.6848	434.5767
	Reddy (2000)	24.1789	75.3751	160.5102	279.2980	431.3412
	Zenkour (2010)	24.1789	75.3753	160.5109	279.3000	431.3459
	Present Theory 1	24.1789	75.3753	160.5109	279.3000	431.3459
	Present Theory 2	24.1790	75.3758	160.5131	279.3063	431.3605
1	CPT	5.5209	27.8683	65.1140	117.2580	184.3002
	Reddy (2000)	5.5138	27.8242	64.9376	116.7490	183.1123
	Zenkour (2010)	5.5138	27.8242	64.9379	116.7498	183.1140
	Present Theory 1	5.5138	27.8242	64.9379	116.7498	183.1140
	Present Theory 2	5.5139	27.8244	64.9387	116.7521	183.1194

Table 8 Continued

P	Theory	$a/b=1$	$a/b=2$	$a/b=3$	$a/b=4$	$a/b=5$
2	CPT	3.5956	22.1916	53.1850	96.5757	152.3637
	Reddy (2000)	3.5893	22.1522	53.0273	96.1209	151.3023
	Zenkour (2010)	3.5893	22.1521	53.0271	96.1203	151.3011
	Present Theory 1	3.5893	22.1521	53.0271	96.1203	151.3011
	Present Theory 2	3.5893	22.1522	53.0275	96.1213	151.3034
5	CPT	3.8999	22.6595	53.9256	97.6980	153.9769
	Reddy (2000)	3.8912	22.6052	53.7086	97.0725	152.5184
	Zenkour (2010)	3.8911	22.6047	53.70.68	97.0673	152.5063
	Present Theory 1	3.8911	22.6047	53.7068	97.0673	152.5063
	Present Theory 2	3.8911	22.6045	53.7058	97.0644	152.4995
10	CPT	4.3757	24.8897	57.3198	103.6459	163.2080
	Reddy (2000)	4.3653	24.1650	57.0615	102.9015	161.4729
	Zenkour (2010)	4.3653	24.1648	57.0607	102.8991	161.4774
	Present Theory 1	4.3653	24.1648	57.0607	102.8991	161.4674
	Present Theory 2	4.3653	24.1649	57.0609	102.8997	161.4689
Metal	CPT	1.0029	17.5072	45.0145	83.5246	133.0377
	Reddy (2000)	0.9967	17.4685	44.8598	83.0785	131.9967
	Zenkour (2010)	0.9967	17.4685	44.8600	83.0791	131.9982
	Present Theory 1	0.9967	17.4685	44.8600	83.0791	131.9982
	Present Theory 2	0.9967	17.4687	44.8607	83.0811	132.0029

Table 9 Critical buckling temperature of square FG plate under linear temperature rise for different values of power law index P and side-to-thickness ratio a/h

P	Theory	$a/h=10$	$a/h=20$	$a/h=40$	$a/h=60$	$a/h=80$	$a/h=100$
Ceramic	CPT	3409.8213	844.9553	203.7388	84.9950	43.4347	24.1982
	Reddy (2000)	3227.3638	833.0705	202.9881	84.8464	43.3876	24.1789
	Zenkour (2010)	3227.6401	833.0879	202.9892	84.8466	43.3877	24.1789
	Present Theory 1	3227.6401	833.0879	202.9892	84.8466	43.3877	24.1789
	Present Theory 2	3228.4506	833.1413	202.9925	84.8473	43.3879	24.1790
1	CPT	1357.7181	335.2421	78.0861	30.0178	13.0479	5.1291
	Reddy (2000)	1412.9608	358.7114	83.4614	31.9522	13.8839	5.5138
	Zenkour (2010)	1413.0711	358.7178	83.4618	31.9523	13.8839	5.5138
	Present Theory 1	1413.0711	358.7178	83.4618	31.9523	13.8839	5.5138
	Present Theory 2	1413.3734	358.7375	83.4630	31.9525	13.8840	5.5139
2	CPT	1065.8296	264.8413	61.8500	23.4694	9.7823	3.3373
	Reddy (2000)	1170.8157	297.2305	68.4355	25.5866	10.5537	3.5893
	Zenkour (2010)	1170.7587	297.2261	68.4352	25.5866	10.5537	3.5893
	Present Theory 1	1170.7587	297.2261	68.4352	25.5866	10.5537	3.5893
	Present Theory 2	1170.8951	297.2347	68.4357	25.5867	10.5537	3.5893

Table 9 Continued

P	Theory	$a/h=10$	$a/h=20$	$a/h=40$	$a/h=60$	$a/h=80$	$a/h=100$
5	CPT	1106.3768	276.0209	65.0910	25.0893	10.7956	4.0568
	Reddy (2000)	1160.6852	298.7050	69.2199	26.0665	10.9135	3.8912
	Zenkour (2010)	1160.0634	298.6611	69.2171	26.0659	10.9133	3.8911
	Present Theory 1	1160.0634	298.6611	69.2171	26.0659	10.9133	3.8911
	Present Theory 2	1159.7240	298.6366	69.2155	26.0656	10.9132	3.8911
10	CPT	1239.0539	307.2174	71.8775	27.6383	11.9548	4.6139
	Reddy (2000)	1218.6392	315.6834	73.4616	27.8265	11.7956	4.3653
	Zenkour (2010)	1218.3724	315.6637	73.4603	27.8263	11.7956	4.3653
	Present Theory 1	1218.3724	315.6637	73.4603	27.8263	11.7956	4.3653
	Present Theory 2	1218.4670	315.6692	73.4607	27.8263	11.7956	4.3653
Metal	CPT	1090.2903	265.0725	58.7681	20.5636	7.1920	1.0029
	Reddy (2000)	1031.5866	261.2487	58.5266	20.5158	7.1769	0.9967
	Zenkour (2010)	1031.6755	261.2543	58.5269	20.5158	7.1769	0.9967
	Present Theory 1	1031.6755	261.2543	58.5269	20.5158	7.1769	0.9967
	Present Theory 2	1031.9362	261.2715	58.5280	20.5161	7.1769	0.9967

Table 10 Critical buckling temperature of FG plate under non-linear temperature rise for different values of power law index k and aspect ratio a/b , and temperature exponent γ with $a/h=10$

P	Theory	$a/b=1$			$a/b=2$			$a/b=3$		
		$\gamma=2$	$\gamma=5$	$\gamma=10$	$\gamma=2$	$\gamma=5$	$\gamma=10$	$\gamma=2$	$\gamma=5$	$\gamma=10$
Ceramic	CPT	5.1147	10.2294	18.7540	12.8093	25.6186	46.9675	25.6336	51.2673	93.9900
	Reddy (2000)	4.8410	9.6820	17.7505	11.2269	22.4538	41.1654	20.0066	40.0133	73.3577
	Zenkour (2010)	4.8414	9.6829	17.7520	11.2294	22.4589	41.1747	20.0164	40.0328	73.3934
	Present Theory 1	4.8414	9.6829	17.7520	11.2294	22.4589	41.1747	20.0164	40.0328	73.3934
	Present Theory 2	4.8426	9.6853	17.7564	11.2363	22.4727	41.1999	20.0401	40.0802	73.4803
1	CPT	2.2072	4.5241	8.5812	5.5391	11.3534	21.5346	11.0921	22.7355	43.1235
	Reddy (2000)	2.1066	4.3179	8.1900	4.9508	10.1476	19.2474	8.9673	18.3802	34.8626
	Zenkour (2010)	2.1067	4.3182	8.1906	4.9517	10.1495	19.2512	8.9711	18.3880	34.8774
	Present Theory 1	2.1067	4.3182	8.1906	4.9517	10.1496	19.2512	8.9711	18.3880	34.8774
	Present Theory 2	2.1072	4.3191	8.1924	4.9543	10.1549	19.2613	8.9804	18.4070	34.9134
2	CPT	1.7627	3.4419	6.4379	4.4256	8.6417	16.1638	8.8640	17.3080	32.3737
	Reddy (2000)	1.6766	3.2738	6.1235	3.9246	7.6633	14.3339	7.0658	13.7970	25.8066
	Zenkour (2010)	1.6765	3.2736	6.1232	3.9243	7.6627	14.3327	7.0654	13.7962	25.8051
	Present Theory 1	1.6765	3.2736	6.1232	3.9243	7.6627	14.3327	7.0654	13.7962	25.8051
	Present Theory 2	1.6767	3.2740	6.1239	3.9255	7.6650	14.3370	7.0700	13.8052	25.8218
5	CPT	1.7083	3.0498	5.3522	4.2885	7.6562	13.4363	8.5888	15.3337	26.9097
	Reddy (2000)	1.5964	2.8500	5.0017	3.6521	6.5202	11.4425	6.3755	11.3822	19.9751
	Zenkour (2010)	1.5955	2.8485	4.9990	3.6479	6.5126	11.4292	6.3635	11.3608	19.9377
	Present Theory 1	1.5955	2.8485	4.9990	3.6479	6.5126	11.4292	6.3635	11.3608	19.9377
	Present Theory 2	1.5950	2.8477	4.9975	3.6457	6.5086	11.4223	6.3572	11.3508	19.9200

Table 10 Continued

P	Theory	$a/b=1$			$a/b=2$			$a/b=3$		
		$\gamma=2$	$\gamma=5$	$\gamma=10$	$\gamma=2$	$\gamma=5$	$\gamma=10$	$\gamma=2$	$\gamma=5$	$\gamma=10$
10	CPT	1.8092	3.1126	5.1492	4.5414	7.8130	12.9250	9.0951	15.6470	25.8848
	Reddy (2000)	1.6770	2.8850	4.7728	3.7970	6.5322	10.8062	6.5402	11.2515	18.6134
	Zenkour (2010)	1.6766	2.8844	4.7717	3.7953	6.5293	10.8015	6.5362	11.2448	18.6022
	Present Theory 1	1.6766	2.8844	4.7717	3.7953	6.5293	10.8015	6.5362	11.2448	18.6022
	Present Theory 2	1.6767	2.8846	4.7721	3.7962	6.5309	10.8040	6.5400	11.2512	18.6128
Metal	CPT	1.6354	3.2708	5.9965	4.1110	8.2221	15.0739	8.2371	16.4743	30.2029
	Reddy (2000)	1.5473	3.0947	5.6737	3.6019	7.2039	13.2072	6.4267	12.8535	23.5647
	Zenkour (2010)	1.5475	3.0950	5.6742	3.6027	7.2055	13.2102	6.4298	12.8597	23.5762
	Present Theory 1	1.5475	3.0950	5.6742	3.6027	7.2055	13.2102	6.4298	12.8597	23.5762
	Present Theory 2	1.5479	3.0958	5.6757	3.6050	7.2100	13.2183	6.4375	12.8750	23.6042

Table 11 Critical buckling temperature of FG plate under non-linear temperature rise for different values of power law index P and aspect ratio a/b , and temperature exponent γ with $a/h=5$

P	Theory	$a/b=1$			$a/b=2$			$a/b=3$		
		$\gamma=2$	$\gamma=5$	$\gamma=10$	$\gamma=2$	$\gamma=5$	$\gamma=10$	$\gamma=2$	$\gamma=5$	$\gamma=10$
Ceramic	CPT	20.5039	41.0078	75.1810	51.2823	102.5646	188.0351	102.4896	205.1592	376.1253
	Reddy (2000)	16.7353	33.4706	61.3626	32.8633	65.7266	120.4989	48.5388	97.0776	177.9756
	Zenkour (2010)	16.7353	33.4833	61.3861	32.8985	65.7971	120.6281	48.6504	97.3080	178.3980
	Present Theory 1	16.7416	33.4833	61.3861	32.8985	65.7971	120.6281	48.6540	97.3080	178.3980
	Present Theory 2	16.7577	33.5154	61.4450	32.9725	65.9451	120.8994	48.8584	97.7169	179.1477
1	CPT	8.8709	18.1827	34.4879	22.1983	45.4997	86.3014	44.4106	91.0281	172.6573
	Reddy (2000)	7.4561	15.2827	28.9875	15.0800	30.9094	58.6274	22.9214	46.9819	89.1127
	Zenkour (2010)	7.4585	15.2878	28.9970	15.0944	30.9390	58.6835	22.9714	47.0843	89.3070
	Present Theory 1	7.4585	15.2878	28.9970	15.0944	30.9390	58.6835	22.9714	47.0843	89.3070
	Present Theory 2	7.4647	15.3005	29.0212	14.1247	31.0011	58.8013	23.0600	47.2659	89.6516
2	CPT	7.0886	13.8415	25.8889	17.7406	34.6407	64.7936	35.4938	69.3061	129.6333
	Reddy (2000)	5.8885	11.4980	21.5065	11.7750	22.9923	43.0059	17.7018	34.5650	64.6519
	Zenkour (2010)	5.8880	11.4971	21.5048	11.7774	22.9970	43.0146	17.7226	34.6058	64.7282
	Present Theory 1	5.8880	11.4971	21.5048	11.7774	22.9970	43.0146	17.7226	34.6058	64.7282
	Present Theory 2	5.8910	11.5030	21.5157	11.7940	23.0294	43.0753	17.7774	34.7127	64.9282

Table 11 Continued

P	Theory	$a/b=1$			$a/b=2$			$a/b=3$		
		$\gamma=2$	$\gamma=5$	$\gamma=10$	$\gamma=2$	$\gamma=5$	$\gamma=10$	$\gamma=2$	$\gamma=5$	$\gamma=10$
5	CPT	6.8687	12.2627	21.5203	17.1895	30.6885	53.8566	34.3909	61.3982	107.7502
	Reddy (2000)	5.3741	9.5945	16.8378	10.1682	18.1534	31.8582	14.5269	25.9349	45.5142
	Zenkour (2010)	5.3654	9.5789	16.8104	10.1426	18.1076	31.7779	14.4932	25.8748	45.4087
	Present Theory 1	5.3654	9.5789	16.8104	10.1426	18.1076	31.7779	14.4932	25.8748	45.4087
	Present Theory 2	5.3611	9.5711	16.7968	10.1335	18.0914	31.7494	14.4953	25.8785	45.4152
10	CPT	7.2736	12.5134	20.7009	18.2025	31.3150	51.8043	36.4172	62.6510	103.6433
	Reddy (2000)	5.5400	9.5308	15.7669	10.2435	17.6226	29.1530	14.3463	24.6810	40.8297
	Zenkour (2010)	5.5369	9.5255	15.7580	10.2387	17.6144	29.1395	14.3554	24.6966	40.8555
	Present Theory 1	5.5369	9.5255	15.7580	10.2387	17.6144	29.1395	14.3554	24.6966	40.8555
	Present Theory 2	5.5392	9.5296	15.7648	10.2532	17.6393	29.1806	14.4038	24.7799	40.9934
Metal	CPT	6.5867	13.1734	24.1513	16.4893	32.9787	60.4609	32.9937	65.9874	120.9769
	Reddy (2000)	5.3742	10.7484	19.7055	10.5632	21.1264	38.7319	15.6066	31.2133	57.2244
	Zenkour (2010)	5.3762	10.7525	19.7130	10.5745	21.1491	38.7734	15.6437	31.2874	57.3603
	Present Theory 1	5.3762	10.7525	19.7130	10.5745	21.1491	38.7734	15.6437	31.2874	57.3603
	Present Theory 2	5.3814	10.7628	19.7319	10.5983	21.1967	38.8607	15.7095	31.4190	57.6015

The critical buckling load is presented in Tables 3, 4 and 5 for a simply supported plate subjected to uniaxial compression, biaxial compression and compression and tension at the same time, respectively. In each table we took three different values of aspect ratio a/b and the thickness ratio a/h , further, the material varies gradually from ceramic to metal. From the tables, it can clearly be observed that the critical buckling load decreases with the increase of the material property P , which is logical since we goes from the more rigid material (which is ceramic) at least rigid material (which is metal). Moreover, the critical buckling load increases with increasing of the thickness ratio a/h and the aspect ratio a/b for all load cases.

Fig. 2 shows the variation of the critical buckling load of a functionally graded plate as a function of the material property P for different values of the aspect ratio a/b using the present theories 1 and 2. From this figure we can pull two important observations: first, the critical buckling load decreases with the increase of the material index P , which is obvious since we graduate from the more rigid material to the less rigid, and second, that this load increases by increasing the aspect ratio a/b . Fig. 3 shows the variation of the critical buckling load of a

functionally graded square plate as function of thickness ratio of a/h for different values of material index P , where the critical load increases quickly in the case of thick plates ($a/h < 20$) and slowly for thin plates ($a/h > 20$). Fig. 4 shows that the critical buckling load of the plate is maximum in the case of ceramic and decreases until the metal where it reaches its minimum value (see also e comparison tables).

Fig. 5 shows the variation of the critical buckling load of a square FGM plate as a function of E_c/E_m ratio for different values of material index P . From the last figure it can be seen that the critical buckling load increases with the increasing of E_c/E_m ratio, that is to say the increase in the percentage of the ceramic increases the critical buckling load in the plate and vice versa.

3.2 Thermal buckling load

In Tables 6 and 7 the results of buckling analysis for the plate under uniform temperature rise are presented. These tables show the comparisons of the critical buckling temperature change obtained by the present theory with those given by Eslami and Samsam (2006) based on both higher plate theory Reddy (2000), Zenkour (2010) and the classical plate theory CPT, The results of the presents theories (present theory 1 and present theory 2) show very good agreement with higher plate theory (Reddy 2000, Zenkour and Sobhy 2010) and thick FGM plates. Table 6 shows that the buckling temperature increases by the increase of the aspect ratio b/a and decreases with increase of the power law index P from 0 to 10. Table 7 shows that the buckling temperature decreases by the increase of the dimension ratio a/h and the power law index P from 0 to 10. It is interesting to note that the buckling temperatures for homogeneous plates ($P=0$) are considerably higher than those for the FGM plates ($P>0$), especially for the comparatively longer and thicker plates. The critical buckling temperatures obtained based on classical plate theory are noticeably greater than values obtained based on higher order shear deformation theory. The differences are considerable for long and thin plates.

In Tables 8 and 9 the results of buckling analysis for the plate under linear temperature change across the thickness are presented. It can be seen that the results of present theory are almost identical with those reported by Javaheri and Eslami (2002) based on Reddy (2000), Zenkour and Sobhy (2010). It is concluded that the buckling temperature increases by the increase of the aspect ratio a/b , decreases by the increase of the power law index P , and decreases by the increase of the dimension ratio a/h . Also, the buckling temperatures for homogeneous plates are considerably higher than those for the FGM plates especially for the comparatively longer and thicker plates. The critical buckling temperatures obtained based on classical plate theory are noticeably greater than values obtained based on higher order shear deformation theory. The differences are considerable for long and thin plates. Hence, in order to obtain accurate results for thick FG plates, it is necessary to consider the transverse shear deformation effects by using shear deformation theories. It should be noted that the unknown function in present theory is only four, while the unknown function in both Reddy (2000), Zenkour and Sobhy (2010) is five. It can be concluded that the present theory is not only accurate but also simple in predicting critical buckling temperature of FG plates.

Tables 10 and 11 exhibit the critical temperature difference $t_{cr} = 10^{-3} T_{cr}$ for different values of the aspect ratio a/b , the temperature exponent γ and the power law index P under non-linear temperature loads at $a/h=10$ and 5, respectively. The nonlinearity temperature exponent γ is taken here as 2, 5 and 10. It can be concluded from the presented results that the present theory gives more accurate results of critical buckling temperature when compared to the higher-order shear

deformation theory. The effect of a/b on the critical buckling t_{cr} is similar to that in the case of uniform and linear temperature difference across the thickness. As the power law index k increases, the critical buckling t_{cr} decreases to reach lowest values and then increases excluding t_{cr} of the rectangular plates for $\gamma=10$. It is also noticed from Tables 10 and 11 that the T_{cr} increases with the increase of the non-linearity parameter γ . In general, the values of the critical temperature difference calculated by using the shear deformation theories are lower than those calculated by using the classical plate theory, indicating the shear deformation effect.

Fig. 6 shows the variation trend of critical temperature difference T_{cr} with respect to the plate aspect ratio a/b for different values of material gradient index P under a uniform, linear and non-linear temperature loads. It is observed that with increasing the plate aspect ratio a/b , the critical buckling temperature difference also increases steadily, whatever the material gradient index P is. Because the ceramic plate is weaker than the metallic one, thus the critical buckling temperature of the first plate is higher than that of the second. For the FGM plate, T_{cr} decreases as the metallic constituent in the plate increases. The critical buckling temperature change T_{cr} versus the side-to-thickness ratio a/h and the aspect ratio a/b of FGM plates under various thermal loading types is exhibited in Figs. 7, 8 and 9. It can be seen from these figures that, regardless of the loading type and the power-law index P , the critical buckling temperature difference T_{cr} decreases as the side-to-thickness ratio a/h increases and it is reduced with the decrease of the aspect ratio a/b . The critical buckling temperature for the ceramic plate is higher than that for the FGM plate. This is because the ceramic plate is stronger than the other. The differences between the loading types decrease with the increase of a/h because the plate becomes thin. It is also noticed from Figs. 8 and 9 that the T_{cr} increases with the increase of the non-linearity parameter γ .

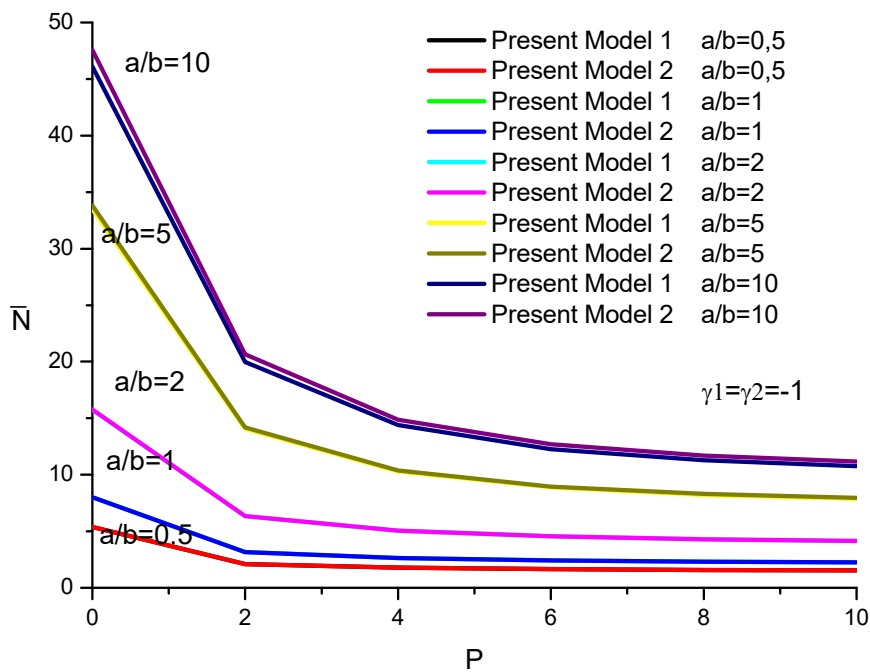


Fig. 2 Variation of the critical buckling load \bar{N} of an FGM square plate of as a function of the material property P for different values of the aspect ratio a/b with $(a=5h)$

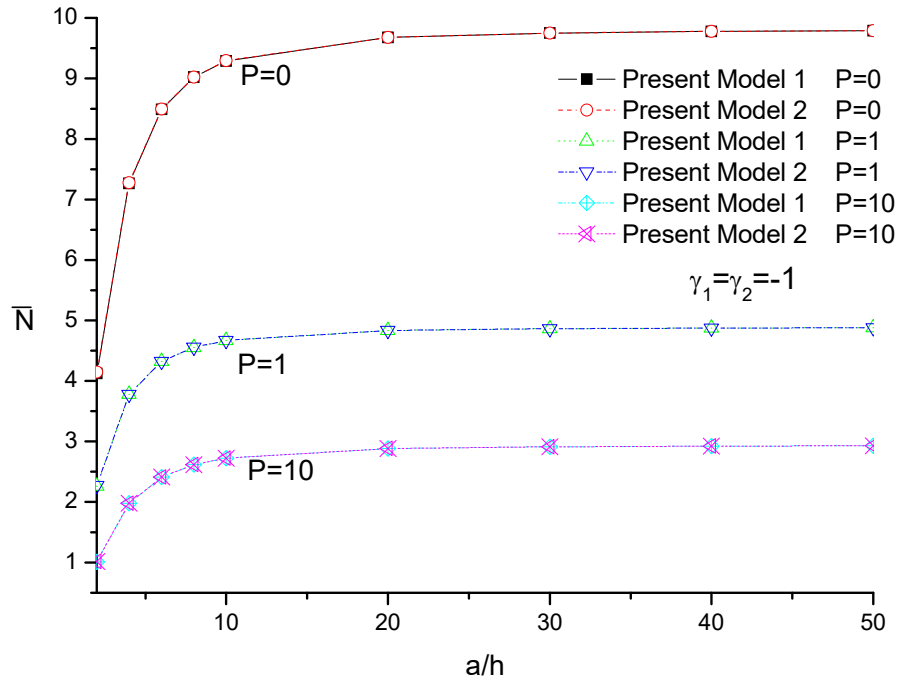


Fig. 3 Variation of the critical buckling load \bar{N} of a functionally graded square plate as a function of thickness ratio a/h

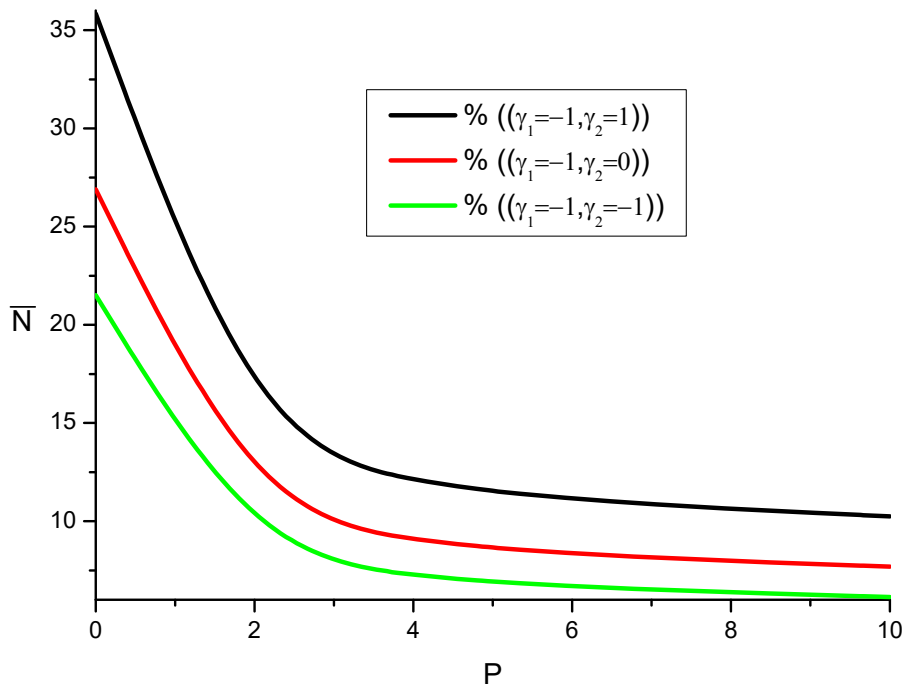


Fig. 4 The effect of the material property P on the critical buckling load for a simply supported square plate ($a=b=10h$) under various loading conditions

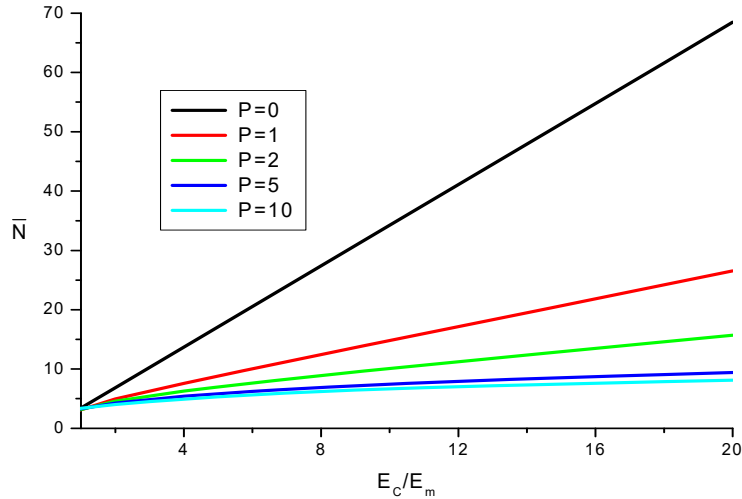


Fig. 5 Effect of the ratio E_c/E_m on the critical buckling load for a simply supported square plate made of FGM ($a=b=10h$) under uniaxial compression ($\gamma_1=-1, \gamma_2=0$)

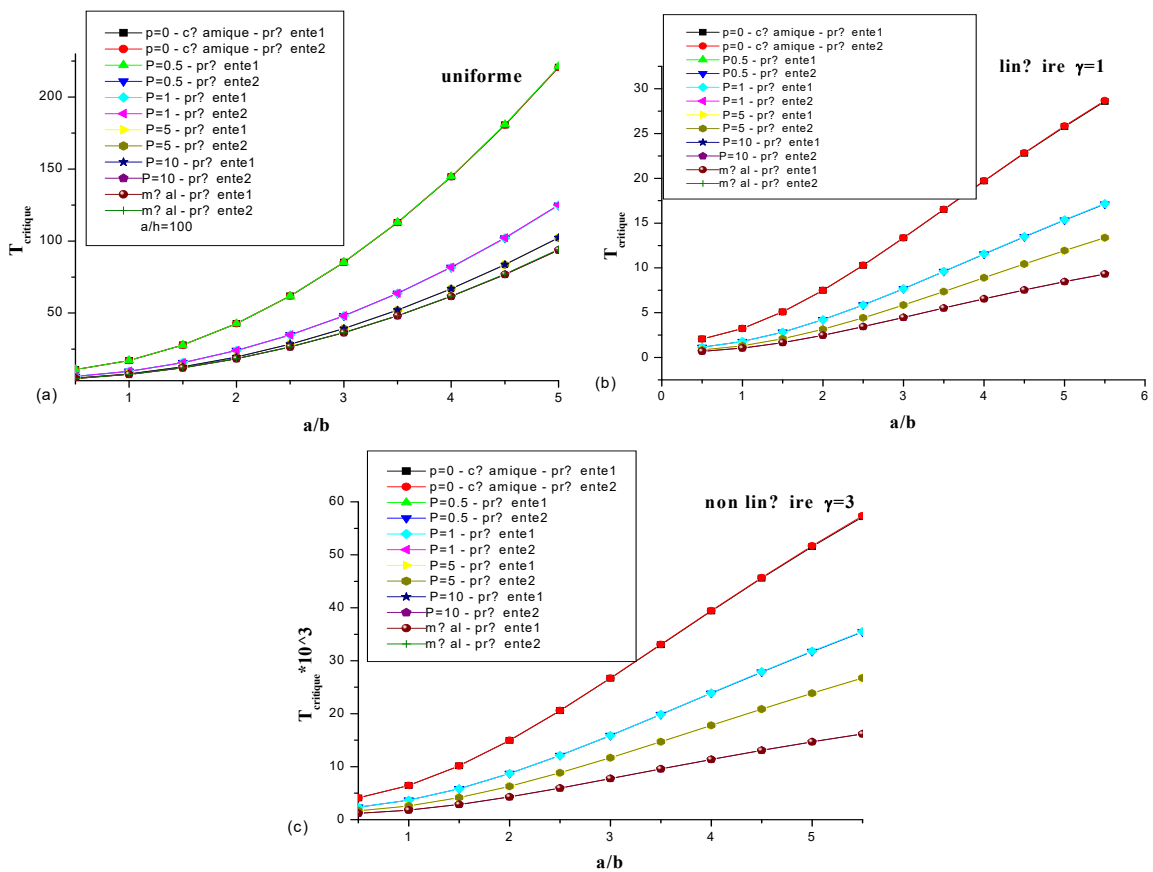


Fig. 6 Critical buckling temperature difference T_{cr} due to uniform (a), linear (b) and non-linear (c) temperature rise across the thickness versus the aspect ratio a/b

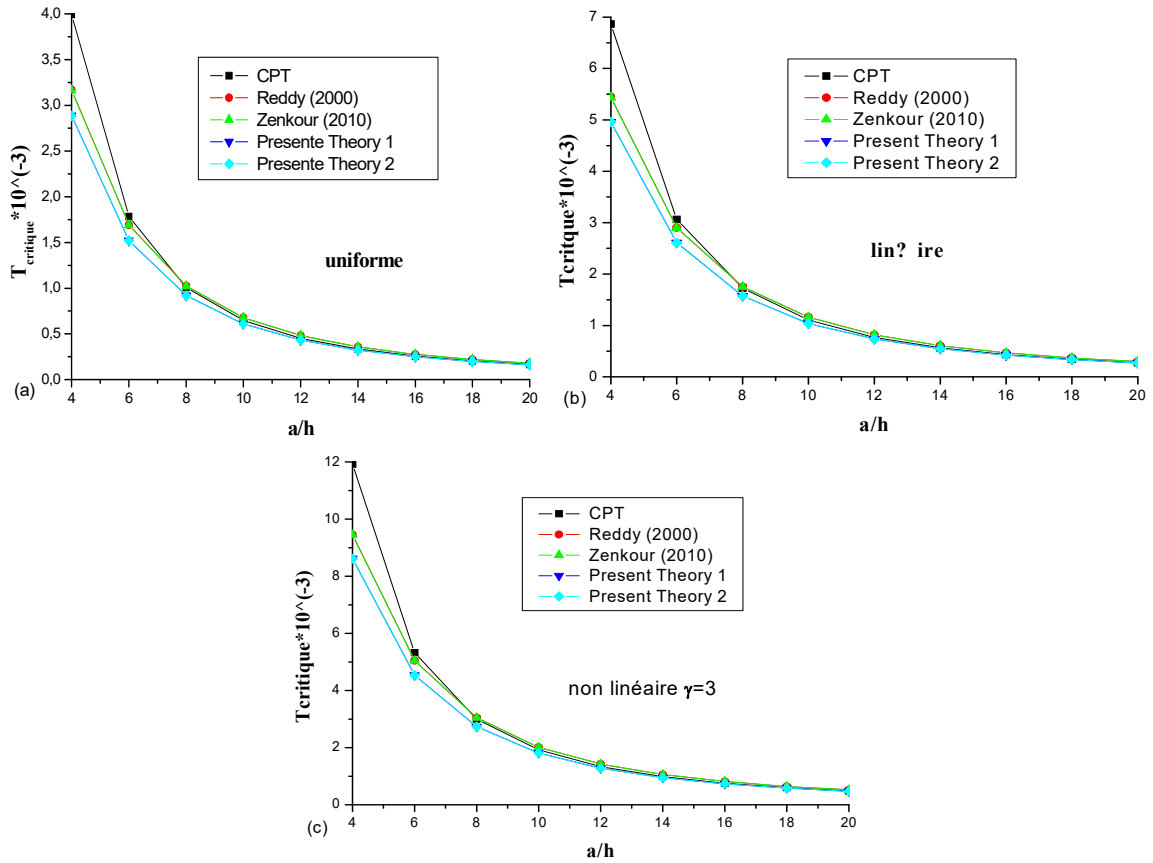


Fig. 7 Critical buckling temperature difference T_{cr} due to uniform (a), linear (b) and non-linear (c) temperature rise across the thickness versus the side-to-thickness ratio a/h

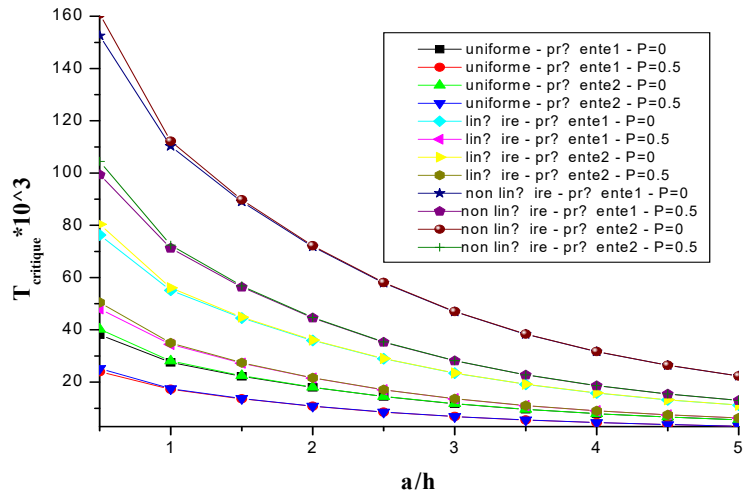


Fig. 8 Critical buckling temperature difference T_{cr} due to uniform, linear and non-linear temperature rise across the thickness versus the side-to-thickness ratio a/h and for different values of the nonlinearity parameter γ ($P=5$)

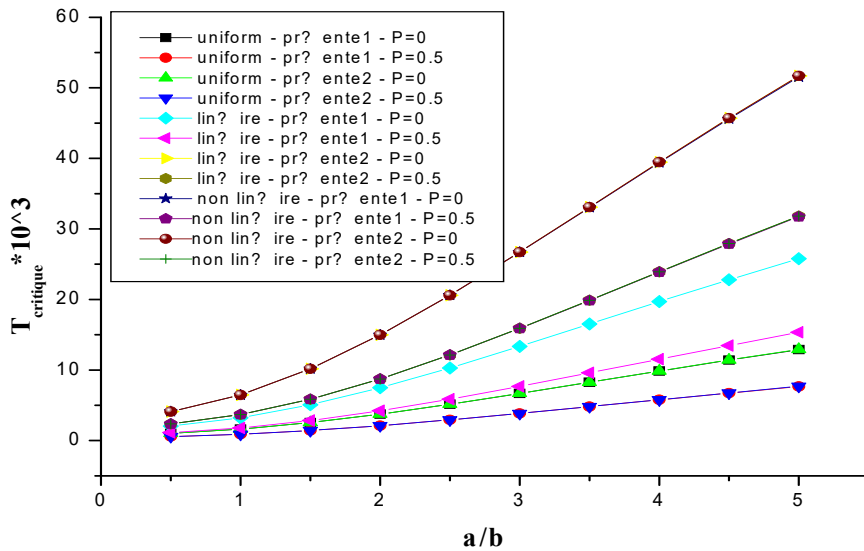


Fig. 9 Critical buckling temperature difference T_{cr} due to uniform, linear and non-linear temperature rise across the thickness versus the aspect ratio a/b and for different values of the non-linearity parameter γ ($P=5$)

4. Conclusions

In this paper, an efficient and simple refined plate theory was successfully developed for buckling analysis of FGM plates. Based on the four variable refined plate theory, the equilibrium and stability equations of thick functionally graded rectangular plates have been derived. The theory, which has strong similarity with classical plate theory in many aspects, accounts for a quadratic variation of the transverse shear strains across the thickness and satisfies the zero traction boundary conditions on the top and bottom surfaces of the plate without using shear correction factors. The accuracy and efficiency of these presents theories have been demonstrated for buckling analysis of simply supported FGM plates. To certify the accuracy of the presents theories, the results obtained by the present analysis have been compared with their counterparts in the literature. It can be concluded that the presents theories is not only accurate but also efficient in predicting the critical buckling loads of FGM plate. Due to the interesting features of the presents theories, the present findings will be a useful benchmark for evaluating the reliable of other future plate theories.

Acknowledgments

The author thanks the referees for their helpful comments.

References

Abdelhak Z., Hadji, L., Hassaine Daouadji, T. and Adda, bedia (2016), "Analysis of buckling response of

- functionally graded sandwich plates using a refined shear deformation theory”, *Wind Struct.*, **22**(3), 291-305.
- Adim, B., Tahar H.D. and Rabahi A., (2016), “A simple higher order shear deformation theory for mechanical behavior of laminated composite plates”, *IJAS, Int. J. Adv. Struct. Eng.*, **8**(2), 103-117.
- Ait Amar Meziane, M., Tounsi, A. and Abdelaziz, H. (2014), “An efficient and simple refined theory for buckling and free vibration of exponentially graded sandwich plates under various boundary conditions”, *J. Sandwich Struct. Mater.*, **16**(3), 293-318.
- Ait Yahia, S., Ait Atmane, H., Houari, M.S.A. and Tounsi, A. (2015), “Wave propagation in functionally graded plates with porosities using various higher-order shear deformation plate theories”, *Struct. Eng. Mech.*, **53**(6), 1143-1165.
- Ahmed, B., Hassen Ait, A., Abdelouahed, T. and Mahmoud, S.R. (2016), “An efficient shear deformation theory for wave propagation of functionally graded material plates”, *Struct. Eng. Mech.*, **57**(5), 837-859.
- Attia, A., Tounsi, A., Adda Bedia, E.A. and Mahmoud, S.R. (2015), “Free vibration analysis of functionally graded plates with temperature-dependent properties using various four variable refined plate theories”, *Steel Compos. Struct.*, **18**(1), 187-212.
- Belabed, Z., Houari, M.S.A., Tounsi, A., Mahmoud, S.R. and Anwar Bég, O. (2014), “An efficient and simple higher order shear and normal deformation theory for functionally graded material (FGM) plates”, *Composites: Part B*, **60**, 274-283.
- Bellifa, H., Benrahou, K.H., Hadji, L., Houari, M.S.A. and Tounsi, A. (2016), “Bending and free vibration analysis of functionally graded plates using a simple shear deformation theory and the concept the neutral surface position”, *J. Braz. Soc. Mech. Sci. Eng.*, **38**(1), 265-275.
- Benferhat, R., Hassaine Daouadji, T. and Mohamed Said, M. (2016), “Effect of porosity on the bending and free vibration response of functionally graded plates resting on Winkler-Pasternak foundations”, *Earthq. Struct.*, **10**(5), 1429-1449.
- Bennoun, M. and Tounsi, A. (2016), “A novel five variable refined plate theory for vibration analysis of functionally graded sandwich plates”, *Mech. Adv. Mater. Struct.*, **23**(4), 423-431.
- Bouazza, M., Abdelouahed, T., Adda-Bedia, E.A. and Megueni, A. (2010), “Thermoelastic stability analysis of functionally graded plates: An analytical approach”, *Comput. Mater. Sci.*, **49**(4), 865-870.
- Bouderba, B., Houari, M.S.A. and Tounsi, A. (2013), “Thermomechanical bending response of FGM thick plates resting on Winkler–Pasternak elastic foundations”, *Steel Compos. Struct.*, **14**(1), 85-104.
- Bourada, M., Kaci, A., Houari, M.S.A. and Tounsi, A. (2015), “A new simple shear and normal deformations theory for functionally graded beams”, *Steel Compos. Struct.*, **18**(2), 409-423.
- Bouderba, B., Houari, M.S.A., Tounsi, A. and Mahmoud, S.R. (2016), “Thermal stability of functionally graded sandwich plates using a simple shear deformation theory”, *Struct. Eng. Mech.*, **58**(3), 397-422.
- Bounouara, F., Benrahou, K.H., Belkorissat, I. and Tounsi, A. (2016), “A nonlocal zeroth-order shear deformation theory for free vibration of functionally graded nanoscale plates resting on elastic foundation”, *Steel Compos. Struct.*, **20**(2), 227-249.
- Bousahla, A.A., Houari, M.S.A., Tounsi, A. and Adda Bedia, E.A. (2014), “A novel higher order shear and normal deformation theory based on neutral surface position for bending analysis of advanced composite plates”, *Int. J. Computat. Method.*, **11**(6), 1350082.
- Chikh, A., Houari, H. and Tounsi, A. (2016), “Thermo-mechanical postbuckling of symmetric S-FGM plates resting on Pasternak elastic foundations using hyperbolic shear deformation theory”, *Struct. Eng. Mech.*, **57**(4), 617-639.
- Cheng, Z.Q. and Batra, R.C. (2000), “Deflection relationships between the homogeneous Kirchhoff plate theory and different functionally graded plate theories”, *Arch. Mech.*, **52**(1), 143-158.
- Eslami, M.R. and Samsam Shariat, B.A. (2006), “Thermal buckling of imperfect functionally graded plates”, *Int. J. Solid. Struct.*, **43**(14), 4082-4096.
- Hamidi, A., Houari, M.S.A., Mahmoud, S.R. and Tounsi, A. (2015), “A sinusoidal plate theory with 5-unknowns and stretching effect for thermomechanical bending of functionally graded sandwich plates”, *Steel Compos. Struct.*, **18**(1), 235-253.
- Hebali, H., Tounsi, A., Houari, M.S.A., Bessaim, A. and Adda Bedia, E.A. (2014), “A new quasi-3D

- hyperbolic shear deformation theory for the static and free vibration analysis of functionally graded plates”, *J. Eng. Mech.*, ASCE, **140**(2), 374-383.
- Houari, M.S.A., Tounsi, A., Bessaim, A. and Mahmoud, S.R. (2016), “A new simple three-unknown sinusoidal shear deformation theory for functionally graded plates”, *Steel Compos. Struct.*, **22**(2), 257-276.
- Hirai, T. and Chen, L. (1999), “Recent and prospective development of functionally graded materials in Japan”, *Mater. Sci. Forum*, **308**, 308-311.
- Javaheri, R. and Eslami, M.R. (2002), “Buckling of functionally graded plates under in-plane compressive loading”, *ZAMM*, **82**(4), 277-283.
- Koizumi, M. (1993), “The concept of FGM”, *Ceramic Trans., Funct. Gradient Mater.*, **34**, 3-10.
- Laoufi, I., Ameer, M. and Zidi, M. (2016), “Mechanical and hygrothermal behaviour of functionally graded plates using a hyperbolic shear deformation theory”, *Steel Compos. Struct.*, **20**(4), 889-911.
- Mahi, A., Adda Bedia, E.A. and Tounsi, A. (2015), “A new hyperbolic shear deformation theory for bending and free vibration analysis of isotropic, functionally graded, sandwich and laminated composite plates”, *Appl. Math. Model.*, **39**(9), 2489-2508.
- Matsunaga, H. (2009), “Thermal buckling of functionally graded plates according to a 2D higher-order deformation theory”, *Compos. Struct.*, **90**(1), 76-86.
- Najafizadeh, M. and Heydari, H. (2008), “An exact solution for buckling of functionally graded circular plates based on higher order shear deformation plate theory under uniform radial compression”, *Int. J. Mech. Sci.*, **50**(3), 603-612.
- Reddy, J.N. (2000), “Analysis of functionally graded plates”, *Int. J. Numer. Meth. Eng.*, **47**(1-3), 663-684.
- Salima, A., Abdelkader, F. and Hayat, S. (2016), “An efficient and simple shear deformation theory for free vibration of functionally graded rectangular plates on Winkler-Pasternak elastic foundations”, *Wind Struct.*, **22**(3), 329-348.
- Sobhy, M. and Zenkour, A.M. (2010), “Thermal buckling of various types of FGM sandwich plates”, *Compos. Struct.*, **93**(1), 93-102.
- Şimşek, M. (2010), “Fundamental frequency analysis of functionally graded beams by using different higher-order beam theories”, *Nuclear Eng. Des.*, **240**(4), 697-705.
- Shimpi, R. (2002), “Refined plate theory and its variants”, *AIAA J.*, **40**(1), 137-146.
- Tanigawa, Y. (1995), “Some basic thermoelastic problems for nonhomogeneous structural materials”, *Appl. Math. Mech.*, **48**(6), 287-300.
- Tounsi, A., Houari, M.S.A. and Benyoucef, S. (2013), “A refined trigonometric shear deformation theory for thermoelastic bending of functionally graded sandwich plates”, *Aero. Sci. Technol.*, **24**(1), 209-220.
- Tounsi, A., Houari, M.S.A. and Bessaim, A. (2016), “A new 3-unknowns non-polynomial plate theory for buckling and vibration of functionally graded sandwich plate”, *Struct. Eng. Mech.*, **60**(4), 547-565.
- Zenkour, A.M. and Mashat, D.S. (2010), “Thermal buckling analysis of ceramic-metal functionally graded plates”, *Nat. Sci.*, **2**(9), 968-978.
- Zidi, M., Tounsi, A., Houari, M.S.A., Adda Bedia, E.A. and Anwar Bég, O. (2014), “Bending analysis of FGM plates under hygro-thermo-mechanical loading using a four variable refined plate theory”, *Aerosp. Sci. Tech.*, **34**, 24-34.
- Zhao, X., Lee, Y.Y. and Liew, K.M. (2009), “Mechanical and thermal buckling analysis of functionally graded plates”, *Compos. Struct.*, **90**(2), 161-171.